Modulational instability and gap solitons in a finite Josephson transmission line

D. Barday and M. Remoissenet
Laboratoire Ondes et Structures Cohérentes (OSC), Faculté des Sciences et Techniques, Université de Bourgogne, 6 Boulevard Gabriel, 21100 Dijon, France
(Received 10 July 1990)

We concentrate on the modulational instability that may develop and perturb the gap soliton or nonlinear standing wave that appears in a finite Josephson transmission line [Phys. Rev. B **41**, 10 387 (1990)] when it has switched to a transmitting state. We first calculate theoretically the spatial dependence of the gap-soliton envelope or nonlinear standing wave inside the system, in terms of Jacobi elliptic functions. Our results fit reasonably well the envelope measured via our computer experiments on the dynamics of the system. Approaching the standing-wave structure in terms of two counterpropagating waves, we show that the evolution of their slowly varying amplitudes can be modeled by two coupled nonlinear Schrödinger equations. Then we calculate the critical wave number and growth rate of the instability for the two counter waves, which is three times larger than the growth rate of either wave alone. The corresponding critical temporal frequency, at which the modulational instability may appear, is in good agreement with the value determined from our numerical experiments.

I. INTRODUCTION

There is currently a great deal of interest in the nonlinear response of physical systems. Particularly, exciting effects due to the nonlinear behavior of systems with artificial gaps, as, for example, modulated structures and superlattices, have been recently investigated.[1–9] In this context, in a recent publication[10] we have examined the transmission properties in the natural gap of a simple system constituted by a Josephson transmission line (JTL) of finite length. We have shown that the nonlinear transmittance exhibits bistability and hysteresis and can approach unity once the amplitude of the incident sinusoidal wave is greater than a certain threshold which is frequency dependent and also decreases with the length of the system. Moreover, a breathing standing wave, which is the so-called gap soliton, appears as soon as the system has switched to a transmitting state. However, in our computer experiments on the dynamics of wave transmission through the JTL we have observed that modulational instability may appear and perturb the dynamical behavior of the gap soliton.

In this paper we concentrate on the gap-soliton envelope and the modulational instability. First, we calculate theoretically the gap soliton envelope. Second, we investigate theoretically the modulational instability conditions in terms of two coupled counterpropagating waves. In both cases our theoretical results are compared with those of our computer experiments.

II. CALCULATION OF THE GAP-SOLITON ENVELOPE

As in our previous paper,[10] we consider a lossless JTL of finite length $\mathcal{L}$ modeled by a continuous electrical transmission line, which is intercalated between two linear nondispersive transmission lines (I) and (III). In the low-amplitude limit the sine-Gordon equation which describes the evolution of the Josephson quantum phase ϕ, can be approximated by

$$\phi_{\tau\tau}-c_0^2\phi_{xx}+\phi-\phi^3/6=0\ , \tag{2.1}$$

where x and τ are scaled space and time variables. The solution of (2.1) may be expressed as a superposition of forward and backward propagation waves of angular frequency ω, wave numbers k^+ and k^-, and slowly varying amplitudes ψ^+ and ψ^- which approximatively obey the following nonlinear dispersion relation:

$$\begin{aligned} k^+&=\frac{1}{c_0}\left[\omega^2-1+\frac{|\psi^+|^2}{2}+|\psi^-|^2\right]^{1/2}\ ,\\ k^-&=\frac{1}{c_0}\left[\omega^2-1+\frac{|\psi^-|^2}{2}+|\psi^+|^2\right]^{1/2}\ . \end{aligned} \tag{2.2}$$

We know that the gap soliton exists as soon as the system has switched to a transmitting state. We limit our calculation of the gap-soliton envelope to the case where the transmittance is unity: $|T|^2=1$ (point Q_2 on Fig. 1); note that Fig. 1 which shows the transmittance of the JTL versus the amplitude $|\psi_{\rm in}^+|$ of the incident wave, corresponds to Fig. 6 in our previous paper. It is reproduced here for the sake of clarity.

We now follow a calculation similar to that used by Chen and Mills[4] for optical systems, to determine theoretically the voltage envelope of the gap soliton (nonlinear standing wave) inside the JTL. We assume that the incoming wave in linear line (I) has frequency ω, wave number k_0, amplitude ψ_0, and velocity $c_0=\omega/k_0$. Then, we look for a stationary solution of Eq. (2.1) of the form

$$\phi(x,\tau)=\psi_0\alpha(x)\exp\{i[\beta(x)-\omega\tau]\}\ , \tag{2.3}$$

where the amplitude $\alpha(x)$ and the phase $\beta(x)$ are real. Upon substituting (2.3) in (2.1), taking account of the boundary conditions at $x=0$ and $x=\mathcal{L}$ and setting $I(x)=\alpha^2(x)$, after calculations similar to Chen and Mills[4] we get

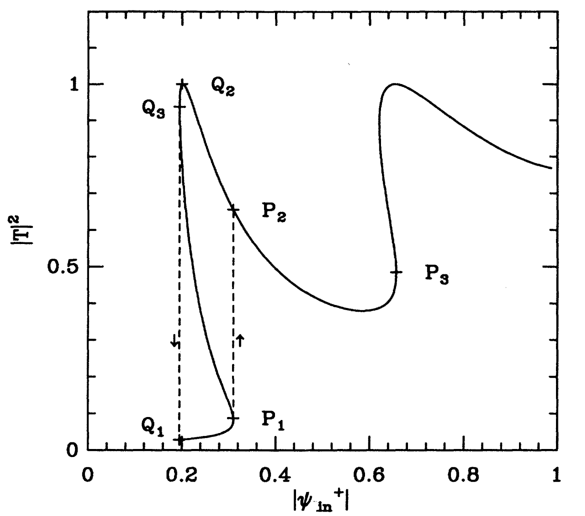

FIG. 1. Representation of the transmittance $|T|^2$ of the JTL vs the amplitude $|\psi_{in}^{+}|$ of the incident wave (see also Fig. 6 in Ref. 10).

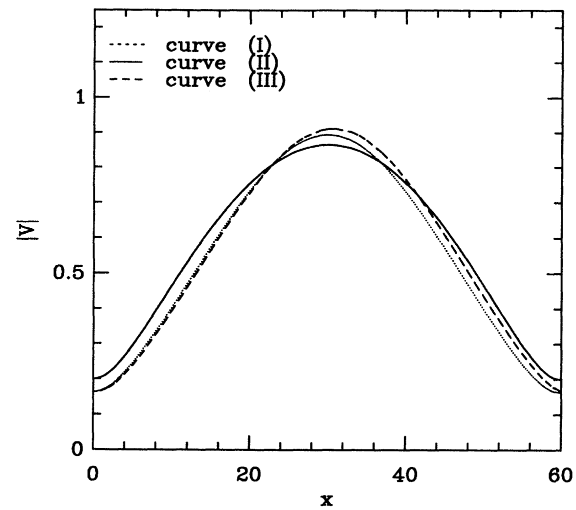

FIG. 2. One period of the gap-soliton envelope represented by the spatial dependence of the modulus $|v(x)|$ of the voltage along the JTL. The theoretical (curve I), experimental (curve III), and the calculated envelope (curve II) are compared.

$$\int_{I(0)}^{I(x)} \frac{dI}{\sqrt{(I^+ - I)(I-1)(I-I^-)}} = \pm \int_0^x \frac{\psi_0}{c_0} dx \ , \quad (2.4a)$$

where

$$I^{\pm} = \frac{1}{2\psi_0^2}(-\psi_0^2 - 4(\omega^2 - 1) \pm \{[\psi_0^2 + 4(\omega^2-1)]^2 + 16\psi_0^2\omega^2\}^{1/2}) \ . \quad (2.4b)$$

We also have the condition $I^- < 1 < I^+$, because we limit our study to small amplitudes $\psi_0 \ll 1$ and to frequencies inside the gap, $\omega < \omega_0 = 1$. The integral on the left-hand side of (2.4) may be expressed in terms of Jacobi elliptic functions with modulus μ:

$$I(x) = \frac{(I^+ - I^-) - I^-(I^+ - 1)\mathrm{sn}^2[\xi(x)|\mu]}{(I^+ - I^-) - (I^+ - 1)\mathrm{sn}^2[\xi(x)|\mu]} \ , \quad (2.5a)$$

where

$$\xi(x) = \frac{\psi_0}{2c_0}(\sqrt{I^+ - I^-})x, \quad \mu^2 = \frac{I^+ - 1}{I^+ - I^-} \ . \quad (2.5b)$$

From expressions (2.5a) and (2.3) we can now calculate $\phi(x)$ which is spatially periodic of period $2K(\mu)$, where $K(\mu)$ is an elliptic integral of first order. Then from the Josephson equation which relates the Josephson phase to the voltage, $v(x,\tau) = \partial\phi/\partial\tau$, we calculate the modulus $|v(x)|$ of the voltage along the JTL, which is represented versus x (curve I) in Fig. 2. Here the parameters are $\omega = 0.99$, $c_0 = 4.47$, and $\mathcal{L} = 60$. We have represented only one period of the gap-soliton envelope inside the JTL which corresponds to state (Q_2) of Fig. 1. For the next switching one will obtain two periods and so on. The theoretical results are compared to those resulting from our numerical experiments on the dynamics of wave transmission through the JTL and also to those we have calculated previously[10] by using the characteristic matrix method (curve II). The theoretical envelope (curve I) fits reasonably well the experimental envelope (curve III). The agreement is not so good when one compares curves II and III: one observes a shift which is attributed to the approximation we have made when using the characteristic matrix method in assuming, by contrast to the above theoretical calculation, that the amplitudes $\psi^{\pm}$ were practically constant inside the JTL.

III. MODULATIONAL INSTABILITY

For numerical experiments, after the JTL has switched to a transmitting state and when the amplitude of the incident wave is further increased to approach a second bistable state (Fig. 1), modulation instability in the Benjamin-Feir sense[11] may occur. Namely, at a given point of the JTL, instead of remaining constant, the amplitude of the voltage becomes instable as time increases. To analyze this modulation instability, we use the multiple-scales perturbation method.[12,13] We assume

$$\phi = \phi_0 + \epsilon\phi_1 + \epsilon^2\phi_2 \ , \quad (3.1)$$

where $\epsilon \ll 1$, and introduce the slow space and time independent variables $x_n = \epsilon^n x$, $\tau_n = \epsilon^n t$. Accordingly, the field $\phi(x,\tau)$ in (2.1) is regarded as $\phi(x_0, x_1, \ldots; t_0, t_1, \ldots)$ and the derivative operators $\partial/\partial x$ and $\partial/\partial\tau$ are expanded in terms of $\partial/\partial x_0$, $\partial/\partial x_1, \ldots$ and $\partial/\partial\tau_0$, $\partial/\partial\tau_1, \ldots$. Then, instead of considering a one-wave stationary solution of the form (2.3) we now look for a solution of (2.1) which is the sum [like that for deriving the nonlinear dispersion relations (2.2)] of two counterpropagating waves with slowly varying amplitudes ψ^+ and ψ^-

$$\phi(x,\tau) = \psi^+(x_1, x_2, \ldots; t_1, t_2, \ldots)\exp(i\theta^+) + \psi^-(x_1, x_2, \ldots; t_1, t_2, \ldots)\exp(i\theta^-) + \mathrm{c.c.} \ , \quad (3.2)$$

where $\theta^+ = kx_0 - \omega t_0$ and $\theta^- = -kx_0 - \omega t_0$, to order ϵ^3

we find the following two coupled amplitude equations:

$$i\left[\frac{\partial\psi^+}{\partial t_2}+V_g\frac{\partial\psi^+}{\partial x_2}\right]+P\frac{\partial^2\psi^+}{\partial x_1^2}+Q(|\psi^+|^2+2|\psi^-|^2)\psi^+=0\ , \quad (3.3a)$$

$$i\left[\frac{\partial\psi^-}{\partial t_2}-V_g\frac{\partial\psi^-}{\partial x_2}\right]+P\frac{\partial^2\psi^-}{\partial x_1^2}+Q(|\psi^-|^2+2|\psi^+|^2)\psi^-=0\ , \quad (3.3b)$$

where V_g is the group velocity, P the group velocity dispersion, Q a nonlinear coefficient:

$$V_g=(k/\omega)c_0^2,\quad P=\frac{1}{2}\left[\frac{\partial\omega}{\partial k}\right]=\frac{c_0^2-V_g^2}{2\omega},\quad Q=\frac{1}{4\omega}\ . \quad (3.4)$$

We are considering frequencies close to the linear cutoff frequency $\omega_0=1$, consequently V_g is small and the terms $V_g(\partial\psi^+/\partial x_2)$ and $-V_g(\partial\psi^-/\partial x_2)$, which are an order of ϵ smaller than derivatives in x_1 may be neglected. It follows that Eqs. (3.3) are approximated by two standard coupled nonlinear Schrödinger (NLS) equations. To simplify the notation, in the following we set $t_2=t$ and $x_1=x$. The modulation instability of copropagating waves with finite amplitude satisfying coupled NLS equations was recently investigated.[14,15] However, here we consider the case of two counterpropagating waves. NLS equations possess equilibrium solutions with constant amplitudes ψ_0^+ and ψ_0^- which are oscillatory in time, given by

$$\phi^+(x,t)=\psi_0^+\exp[i(Q|\psi_0^+|^2+2Q|\psi_0^-|^2)t]\ , \quad (3.5a)$$

$$\phi^-(x,t)=\psi_0^-\exp[i(Q|\psi_0^-|^2+2Q|\psi_0^+|^2)t]\ . \quad (3.5b)$$

To investigate the stability of solutions (3.5) we consider small perturbations ψ_p^+ and ψ_p^-, K_p^+ and K_p^- around their amplitudes and phases:

$$\phi^+(x,t)=(\psi_0^++\psi_p^+)\exp\left[i(Q|\psi_0^+|^2+2Q|\psi_0^-|^2)t+i\int K_p^+(x,t)dx\right]\ , \quad (3.6a)$$

$$\phi^-(x,t)=(\psi_0^-+\psi_p^-)\exp\left[i(2Q|\psi_0^+|^2+Q|\psi_0^-|^2)t+i\int K_p^-(x,t)dx\right]\ . \quad (3.6b)$$

We substitute Eqs. (3.6) in the NLS equations and after some calculations we find that small perturbations of the equilibrium evolve according to the linearized equations

$$(\psi_p^+)_{tt}+P^2(\psi_p^+)_{xxxx}+2QP|\psi_0^+|^2(\psi_p^+)_{xx}+4QP\psi_0^+\psi_0^-(\psi_p^-)_{xx}=0\ , \quad (3.7a)$$

$$(\psi_p^-)_{tt}+P^2(\psi_p^-)_{xxxx}+2QP|\psi_0^-|^2(\psi_p^-)_{xx}+4QP\psi_0^-\psi_0^+(\psi_p^+)_{xx}=0\ . \quad (3.7b)$$

In order to look under which conditions the perturbations will become instable, i.e., will grow exponentially with time with linear growth rate σ, we assume a general solution of the form

$$\psi_p^{\pm}=\exp(i\chi x+\sigma t)\ , \quad (3.8)$$

where χ is the wave number of the perturbation. Substituting (3.8) in (3.7) provides a set of two homogeneous

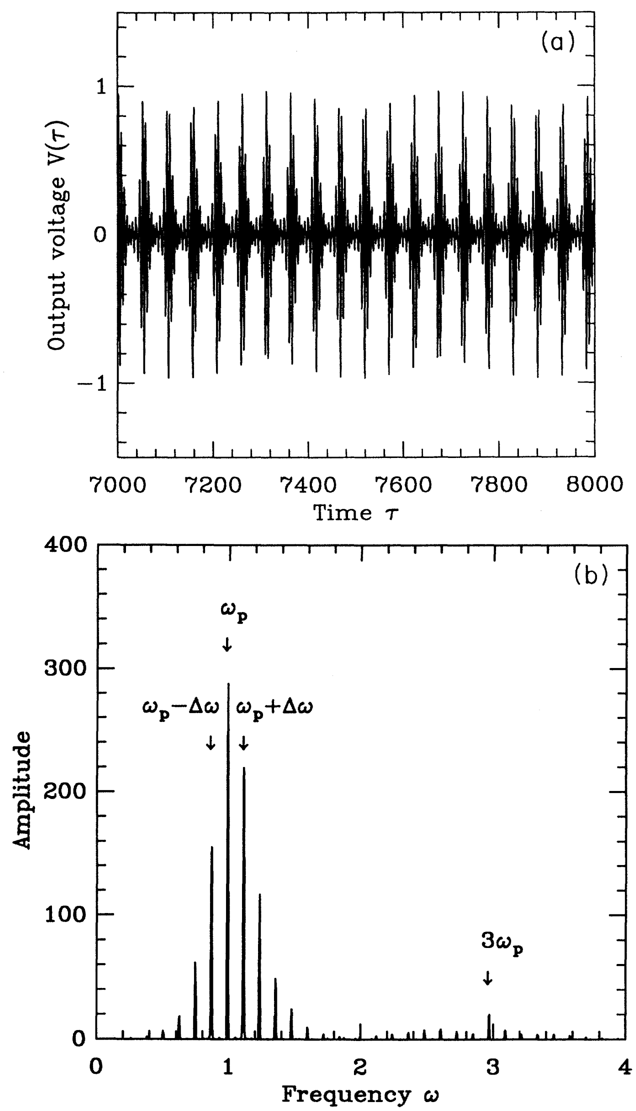

FIG. 3. (a) Representation of the voltage V vs time τ when modulational instability develops as a function of time at a given point of the JTL. Note that as a result of the digital sampling the maximum amplitude, which is constant and equal to one, seems to be modulated. (b) Fourier spectrum showing the lateral peaks at frequencies $(\omega+\Delta\omega)$ and $(\omega-\Delta\omega)$ which corresponds to the modulation observed in (a). Note that the third harmonic at $3\omega_p$ is small.

equations, which have nontrivial solutions only if the determinant of the coefficient matrix vanishes. We finally obtain the maximum growth rate and the corresponding critical wave number which are, respectively, given by

$$\sigma_c = \frac{\Delta^+}{2}, \quad \chi_c^2 = \frac{\Delta^+}{2P}, \tag{3.9}$$

where

$$\Delta^+ = Q(|\psi_0^+|^2 + |\psi_0^-|^2) + [Q^2(|\psi_0^+|^2 - |\psi_0^-|^2)^2 + 16Q^2(\psi_0^+\psi_0^-)^2]^{1/2}. \tag{3.10}$$

To simplify and to compare in the following with our numerical experiments we now assume that the two counterpropagating waves have the same wave number $k = k^+ = k^-$. Under these conditions, relations (2.2) reduce to

$$\omega^2 = 1 + c_0^2 k^2 - \tfrac{3}{2}|\psi_0|^2 \tag{3.11}$$

with $|\psi_0|^2 = |\psi_0^-|^2 = |\psi_0^+|^2$. Then, using the expression of Q given in (3.4), and replacing (3.11) in (3.10), from (3.9) we obtain

$$\sigma_c = \frac{3}{4\omega}|\psi_0|^2, \quad \chi_c^2 = \frac{3}{2(c_0^2 - V_g^2)}|\psi_0|^2. \tag{3.12}$$

At this point it is important to note that if $|\psi_0^-| = 0$, relations (3.9) reduce to the well-known relation which gives the instability growth rate for one wave alone, $\sigma_c = |\psi_0^+|^2/4\omega$. It follows that the growth rate of two counter waves is three times larger than the growth rate of either wave alone.[16]

We now turn our attention to the manifestation of modulation instability in our dynamical simulation experiments in connection with the preceding theoretical results. If a sinusoidal wave of frequency ω_p is launched at the input of the JTL modulational instability generally develops in time at a given point, as represented on Fig. 3(a), when the state of the system approaches the second bistable state (point P_3 on Fig. 1). In fact, for this state the amplitude and consequently σ_c [given by (3.12)] are large enough. Moreover, the discontinuity created by the first switching, in the amplitude $|\psi_{\text{in}}^+|$ of the incident wave, has a Fourier spectrum rich in harmonics. Among all these harmonics the system will select more likely the harmonic with a spatial frequency corresponding to χ_c, and modulational instability will develop. To the critical spatial frequency corresponds a temporal frequency ω_c which is approximated by $\omega_c = \chi_c V_g$. We have performed a numerical experiment with a JTL of length $\mathcal{L} = 120$ unit cells; the parameters of the incident wave are $c_0 = 8.94$, $\omega = \omega_p = 0.99$, $|\psi_{\text{in}}^+| = 0.68$. The corresponding value of k is first determined by measuring the wavelength of the incident wave, when in the experiment modulational instability has not yet appeared. Under these conditions we find $k = 0.039$. Then, using (3.4) and (3.11), we get successively $V_g = 3.17$, $|\psi_0^+| = 0.31$ and the theoretical value of the frequency at which modulational instability may appear is $\omega_c = 0.143$. When modulation instability occurs, the experimental value of the critical frequency can be determined from the Fourier spectrum of the self-modulated wave, as represented in Fig. 3(b). Note that as a result of the digital sampling, the Fourier spectrum seems to be asymmetric. We find $(\omega_c)_{\text{exp}} = \Delta\omega = 0.120$. With respect to the approximations we have made, the agreement between theory and computer experiment is rather good.

IV. CONCLUSION

Following a method similar to that used by Chen and Mills[4] for optical systems, we have calculated theoretically the spatial dependence of the voltage envelope of the low-amplitude gap soliton or nonlinear standing wave inside the JTL, in terms of Jacobi elliptic functions. The theoretical envelope fits reasonably well the experimental envelope measured via our computer experiments on the dynamics of the system.

Approaching the standing wave structure in terms of two counterpropagating waves, we have shown that the evolution of their slowly varying amplitudes can be modeled by two coupled NLS equations. Then, we have calculated the modulational instability conditions, i.e., the growth rate and the corresponding critical wave number. These results, which show that the growth rate of two counter waves is three times larger than the growth rate of either wave alone, allowed us to predict the critical temporal frequency, at which the modulational instability may appear, which is in good agreement with the value measured from our numerical experiments. It suggests that modulational instability, which may perturb the gap-soliton envelope and the dynamics of the system, should be considered carefully in real experiments.

[1] F. Delyon, Y-E. Lévy, and B. Souillard, Phys. Rev. Lett. **57**, 2010 (1986).

[2] W. Chen and D. L. Mills, Phys. Rev. Lett. **58**, 160 (1987).

[3] D. L. Mills and S. E. Trullinger, Phys. Rev. B **36**, 947 (1987).

[4] W. Chen and D. L. Mills, Phys. Rev. B **36**, 6269 (1987).

[5] G. S. Agarwal and D. Gupta, Opt. Lett. **12**, 829 (1987).

[6] D. N. Christodoulides and R. I. Joseph, Phys. Rev. Lett. **62**, 1746 (1989).

[7] J. Coste and J. Peyraud, Phys. Rev. B **40**, 12 201 (1989).

[8] C. M. de Sterke and J. E. Sipe, J. Opt. Soc. Am. B **6**, 1722 (1989).

[9] P. Hawrylak and M. Grabowski, Phys. Rev. B **40**, 8013 (1989).

[10] D. Barday and M. Remoissenet, Phys. Rev. B **41**, 10 387 (1990).

[11] T. B. Benjamin and J. F. Feir, J. Fluid. Mech. **27**, 417 (1967).

[12] T. Kawahara, J. Phys. Soc. Jpn. **35**, 1537 (1973).

[13] R. K. Dodd, J. C. Eilbeck, J. D. Gibbon, and H. C. Morris, *Solitons and Nonlinear Wave Equations* (Academic, London, 1984).

[14] C. J. MacInstrie and R. Bingham, Phys. Fluid B Plasma Phys. **1**, 230 (1989).

[15] G. P. Agrawal, Phys. Rev. A **39**, 3406 (1989).

[16] A. C. Newell, *Solitons in Mathematics and Physics* (Society for Independent and Applied Mathematics, Philadelphia, 1985).